Evaluation of electronic and geometric properties of nanoparticles using X-PEEM

O. Seifarth

IHP-Microelectronics, Im Technologiepark 25, 15236 Frankfurt / Germany
email corresponding author: seifarth@ihp-microelectronics.com

The determination of electronic, geometric and lateral properties of advanced nanocompounds consisting of transition metal oxide nanoparticles or conducting polymers will be presented in detail by using a photoelectron emission microscope in combination with synchrotron radiation (X-PEEM). Making advantage of different contrast mechanism, such as work function differences, chemical bonds and geometric effects, a PEEM allows a quick characterisation. In combination with tunable synchrotron radiation, X-PEEM emerged to one of the few experimental techniques in condensed matter science, allowing a complete determination also of electronic and geometric properties by probing side specific unoccupied densities of states.

Keywords Photoelectron emission microscope; Synchrotron radiation; Spectro-microscopy.

1. Introduction

In the last decades, photoemission electron microscopy (PEEM) performed with x-ray synchrotron radiation (X-PEEM) has emerged to one of the few surface science imaging techniques, which provides a detailed view into the complex properties of advanced materials. Not only the evaluation of lateral structures is possible, even chemical, electronic or magnetic behaviour can be monitored [1]. Contrasting possibilities provided by transmission electron microscopy (TEM) with energy loss filters and ultra high lateral resolution below 1 nm [2], the sample preparation for PEEM experiments is simple and non-destructive with similar information contents. This advantage is paid by the use of synchrotron radiation (SR). Modern SR-sources like BESSY II (Berlin / Germany) or ALS (Berkeley / USA), to name only two, provide tunable photon energies with high energy resolution, high flux, high brilliances and perfectly polarized photons (linear or circular) on a sample spot, not bigger than few microns. Making use of these possibilities, X-PEEM is ideally suited to monitor larger nanostructures, even when they hidden in complex materials [3,4]. Only a different chemical bond which changes the local side specific geometry or coordination or chemical compositions a little bit is sufficient, especially when the exiting photon energy can be tuned.
This chapter is organized as follows: An introduction into the basic principles of an X-PEEM and the desired spectroscopy techniques, x-ray absorption spectroscopy, will be given. Afterwards examples for different contrast mechanism for transition metal oxide nanoparticles and conducting polymers are analysed.

2. Basic principles

When a photon with energy above the work function of a sample impinges on a surface, the excited electron leaving the sample not only possesses a kinetic energy and an emission angle. It emerges from one specific location at the surface. If we now try to detect the electron with an electron microscope a spatial resolved full field image can be obtained. Figure 1 displays the experimental realisation of such an instrument [5]. It has to be stated out here, that the excitation of electrons for PEEM application is not limited to special light sources. Although, in this publication the term x-rays or synchrotron radiation is

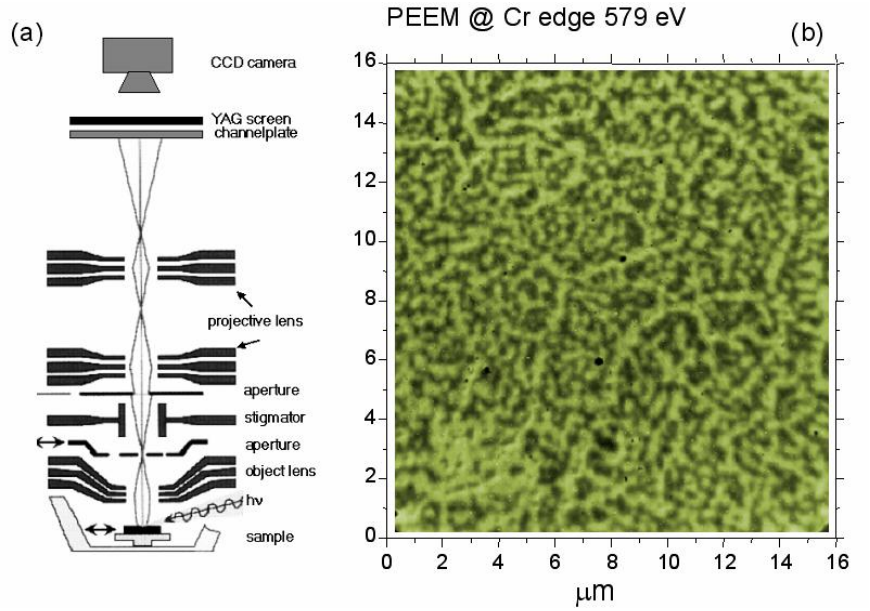

Fig. 1 Basic experimental set up used for X-PEEM in (a). X-PEEM image of a chromium oxide nanowire arrays embedded into a polymer template in (b). The image was taken in the chromium LIII resonance with a photon energy of 579 eV. Due to the lower work function of the metal oxide with respect to the polymer, the nanowire arrays emit more electrons with respect to the polymer and appear brighter. The PEEM image was recorded at the undulator based U49/2 PGM 2 beamline at BESSY II.

mentioned, PEEM becomes also possible by using deuterium, quicksilver, helium discharge lamps or all other light sources, delivering high intensity photons with energies above the work function of the sample.

To allow a lateral scanning mode with our modified Focus IS-PEEM, the sample is mounted on a holder, movable with a piezo-driven motor into the x- and y-direction. Therefore it is possible to scan a sample on various length scales and positions with a PEEM. From several centimetres down to few microns can be down within few minutes, not accessible with a scanning force microscope. One image takes about 0.1 sec. The z-direction is kept fixed during the measurements and the normal distance between sample surface and the first electrostatic lens is about 0.2 cm. The electrons emitted from the sample under x-ray illumination are accelerated with a high extractor voltage of about 3 x 10^6 V/m into the objective lens. By the use of several electrostatic lenses and projector lenses, the picture passes an aperture. It is widened up and sent to a multichannel plate. Here, the electrons are multiplied by several orders of magnitude and send to a phosphorous screen, from which the luminescence is monitored via a CCD camera and send digitalized to the experiment control computer.

The energy resolution for spectroscopy is determined by the photon energy resolution of the beamline or the light source only. The spatial resolution of the PEEM images is limited by three factors derived from the electron optics in the experiments:

- spherical aberration
- chromatic aberration
- diffraction

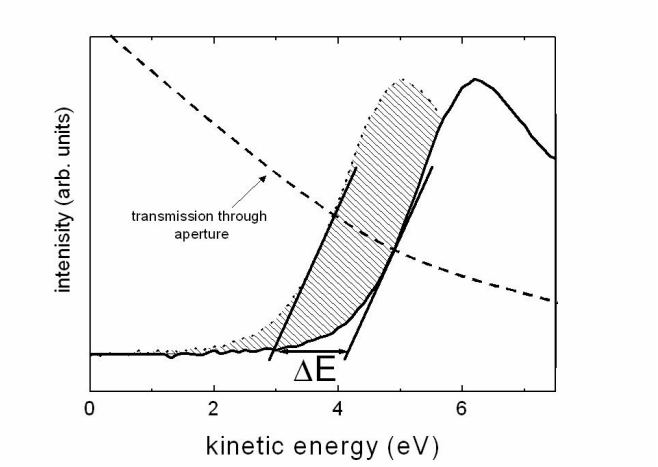

Fig. 2 Sources of work function contrast in X-PEEM. Two electron energy distribution curves from excited electrons are shown for low kinetic energies. Both have different work functions. The transmission curve of a PEEM is also displayed.
Here, the work function difference is around 1 eV, but even very small derivations can be imaged with a PEEM, because of the nearly exponential decay like transmission of the aperture.

In the normal operation mode the chromatic aberration of the accelerating field between sample and electron optics dominate the picture and is therefore the major resolution limiter. Errors in the focussing of electrons with different kinetic energies lead to these aberrations [3;4]. But not all electrons emitted from the sample influence the PEEM image the same way. As seen in figure 2 the number of electrons which take part in the picture developing process is limited. Only those, which are located in the inelastic tail of the energy distribution of the electrons, are transmitted through the aperture [6]. The "slow" electrons, which undergo multiple scattering processes until they leave the sample, exhibit kinetic energies between 0-20 eV and have a sampling depth of 2-10 nm for most K and L edges of transition metals and organic materials [7,8].

For our example, introduced in figure 1(b) with chromium oxide nanowire arrays embedded into polymers, this implies that the electrons from the complete spectral range from 0-579 eV are excited and leave the sample, but only those with low kinetic energies appear in the detector because of discrimination of the aperture [9;10]. This is further discussed in the subsection of work function contrast. The total spatial resolution, which can be obtained with these kinds of PEEMs is around 20 nm [1].

In order to obtain a desired PEEM image which is displaying surface features, the sample must be composed of structures leading to contrast. Two contrast mechanisms are discussed for PEEM and will be summarized below.

- The topographic contrast

If topographic features appear at the surface, the electron trajectories get distorted and peaks appear darker and valleys appear brighter than in flat regions. The angle of incidence of the illumination can also cause contrasts. Surface structure, like flanks directed towards the light source, absorb more photons and appear lighter than those areas which are not illuminated on the opposite side.

- The work function contrast

Another source for contrast in PEEM images is associated to the physical properties of the materials. Changes in the work function can cause large contrasts, because more electrons can be excited. When a

sample is composed of two species with different work function A and B, a light source with a photon energy between A and B can be used. If A is larger than B, areas with the work function A excite electrons and appear bright, areas with the work function B stay dark. If the light source delivers photons slightly higher than both work functions, normally the material with the lower work function will appear brighter than the other. But work function contrast with X-PEEM becomes also possible, when the applied photon energy is hundreds of electron volts higher. This becomes clear when discussing the transmission function of the aperture.

Changing work functions are best seen at the inset of each energy distribution of electrons on the low kinetic energy side [11]. In figure 2 two materials have different work function and the inset of the one with the lower value shift to lower kinetic energies. The transmission function of a PEEM has a maximum for low kinetic energy electrons and decreases nearly exponential over the next tens of electrons. At 20-30 eV the transmission is nearly zero. Therefore, those electrons shown here in the shadowed area contribute more to the PEEM image than all electrons on the right hand side. Therefore it is possible to monitor work function changes even with x-ray source. A nice example of monitoring work function contrast with high photon energies is presented in figure 1(b), where nanowire arrays of chromium oxide appear bright in X-PEEM even with exciting photon energies above 500 eV [10]. The difference in the work function between the transition metal nanostructures and the polymer template, the metal is embedded into, is only 0.2 eV [9,12].

3. Spectro-microscopy combining X-PEEM and μXAS

To fully exploit the possibilities of a PEEM, the usage of synchrotron radiation is required. With the help of tuneable x-rays the element specific properties combined with the spatial resolution down to few tens of nanometers leads to unique insides into matter. When a PEEM is combined with μXAS, x-ray absorption spectroscopy on the micrometer scale, the spectro-microscopy approach is feasible.

3.1 X-ray absorption spectroscopy

X-ray absorption spectroscopy is an experimental technique based on the changes in the absorption cross of a material. It probes the unoccupied electronic structures and densities of states (DOS) and evaluates magnetic and structural properties of the sample under investigation [13]. Among the interactions of light with matter the photo effect, scattering and the creation of electron-positron pairs were reported. For (soft) x-rays (100-2000 eV), the latter is not possible and scattering decays into elastic Thomson scattering and inelastic Compton or Raman scattering. Although scattering processes are present in soft x-ray investigations, the photoelectric absorption is stronger by about three orders of magnitude [14].
If now the sample is irradiated with monoenergetic x-rays delivered from a tunable light source like a synchrotron, the absorption signal decreases continuously when the photon energy is scanned. If the photon energy is large enough to excite an electron from a core hole into the unoccupied states above the Fermi energy or into the continuum states the absorption increases step wise and forms the so called “absorption edges” [7].

At the high energy side of the absorption edges we can distinguish between three ranges:

- The first 10 eV above the absorption edge are called the “edge region”.
- 50-80 eV above the photoionisation energy are defined as “x-ray absorption near edge structure” (XANES).
- At higher energies single scattering of emitted electrons with the neighbouring atoms are observed and this regime is named “extended x-ray absorption fine structure” (EXAFS).

Depending on the core level the absorption edges are labelled in agreement to the notation from Sommerfeld. Transition from 1s levels are named K edges, 2s and 2p levels form the L edges and 3s and 3p are called M edges. Because XAS is referred to be a unique direct probe of the orbital angular moment with quantum number l and its z component m_l of the local unoccupied density of states (DOS)

it must normally follow the dipole selection rules [13]. The dipole selection $\Delta l = \pm 1$ for the transition from a core level with well defined l_i select only those states with $l = l_i \pm 1$.

The K edge spectra corresponds to a 1s—εp transition, therefore the *l = 1* final state is probed and the signal reflects the unoccupied p-like density of states.
For L_{III} edges the transitions can decay into two absorption channels which are dipole allowed.

- 2p—εd transitions, probing the *l = 2* final state with the unoccupied d-DOS
- 2p—εs transitions, probing the *l = 0* final state with the unoccupied s-DOS

For the latter the transition rate probability becomes one or two orders of magnitude lower, therefore the L edges of the transition metals are mainly of d-character.

As seen in the above section on x-ray absorption spectroscopy, probing of electronic and geometric features becomes feasible when scanning the photon energies through the absorption thresholds of the elements. By using the absorption signal, or effects which are closely related to the absorption process, a PEEM can also be used to obtain XAS signals. Among the associated signals suitable for XAS, the fluorescence and the electron yield are most common. The aperture of the PEEM allows only those electrons to pass, which exhibit low kinetic energies. But these are the most important charge carriers for XAS, and it was shown by several groups, that the resulting spectra are intimately related to the absorption of the sample [15].

When X-PEEM experiments are performed, spatial resolved images of the sample surface are recorded for different photon energies. When the photon energy step-widths is decreased and a PEEM image is taken for every step, the fluorescence signal in the CCD camera derived from the emitted electrons can be used as XAS probe. The intensity variations on the phosphorous screen, when the photon energy is scanned through the absorption thresholds, correspond to the electron yield. Therefore each PEEM image can be interpreted as one single spatial resolved data point in XAS. When a set of several PEEM images is recorded on the same sample position for several photon energies, the intensity in the CCD camera can be read out pixel by pixel and plotted versus photon energy. The resulting dataset of 1300 x 1030 data points per photon energy in twelve grey scales in our case can be read out for every pixel, or more appropriate areas with different sizes, and constitute the basis for μXAS with PEEM. The spatial resolution corresponds to the spatial resolution of each PEEM image and is normally in the 50 nm range. Often, the spatial resolution of μXAS is limited by the available photon flux and the emitted electrons per area.

3.2 X-PEEM and μXAS applications on conducting polymers

In figure 3 an example of X-PEEM and μXAS is presented for the conducting polymer polyaniline to resolve agglomerations of nanoparticles genuine to formation during synthesis [5]. One major problem in the field of conducting organic material is the strong sensitivity of the conductivity on the synthesis procedure. Often, samples end up with disappointing electrical performances or chemical stability with unknown origin. In the following investigation the granular structure of polyaniline was found to consist of particles with different chemical environments on a micrometer scale.

In figure 3 X-PEEM images of the conducting polymer polyaniline are shown for different photon energies, 280; 285; 286 and 297 eV, what corresponds to the C K edge regime. The overall intensity variations are clearly resolved from dark (a), to very bright (d). In the picture two areas (1;2) were displayed. From these areas, the μXAS data was extracted and depicted below. Both spectra derived from the brighter area 1 and the darker area 2 clearly show the XAS C K signal, typical for conducting polymers with its different π* and σ* orbitals derived states [16]. Below the C K edge a pre-edge structure is observed, which belongs to the formation of a bipolaron (bp) [17]. Although both areas are only separated by few micrometers, their electronic structure differs significantly as shown in a dramatic increase in one π* state 293 eV photon energy. This difference is attributed to the formation or non-formation of carbon-nitrogen bonds, which are hints for an incomplete synthesis procedure. Because these states and bonds act as the driving forces of the conducting process in polyaniline, the lateral

resolved study on the chemical and electronic structure may lead to improved and more homogeneous thin films.

One explanation of the poor conductivity of some polyaniline films can be extracted from these images shown in figure 3. When the film is consisting of these inhomogeneous distributed grains with differently formed carbon-nitrogen bonds, the large scattering probability at the grain boundaries hinders the charge carriers to penetrate through the film and the overall conductivity decreases.

From the example shown in figure 3, the useful application of a PEEM becomes clear to understand the electronic and chemical structures of matter on a lateral (sub)micrometer scale.

In summary for this example, different chemical states on the micrometer scale lead to a contrast in PEEM and are resolved here with μXAS.

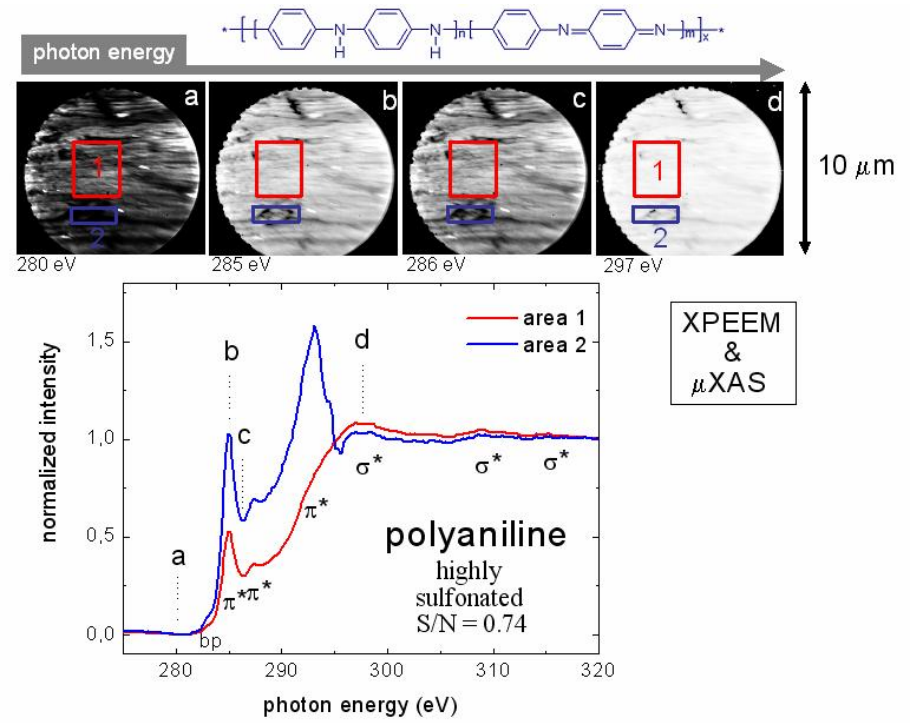

Fig. 3 X-PEEM and μXAS on the conducting polymer polyaniline. The four PEEM images a-d were recorded for different photon energies. For the μXAS data the intensity of the areas 1 and 2, displayed by the boxes, was taken and plotted versus photon energy, when the energy was scanned through the C K edge. Peaks were labelled according to their orbital origin. The spatially resolved XAS spectra were recorded from areas below 2 μm. Smaller spot sizes are also possible in the range around 50 nm, but then the intensity for the XAS spectra drastically decreases. The structure of the conducting polymer polyaniline is displayed in the upper inset, more explanations are given in the text.

3.3 X-PEEM and μXAS on standing chromium nanorod arrays embedded into block copolymers

One of the important questions in research on transition metal (oxide) nanoparticles is how physical properties change with downsizing and what are unique effects with respect to their bulk counterparts? In the following example with standing chromium nanorods in polymer templates, we will present an approach to handle the above question with X-PEEM.

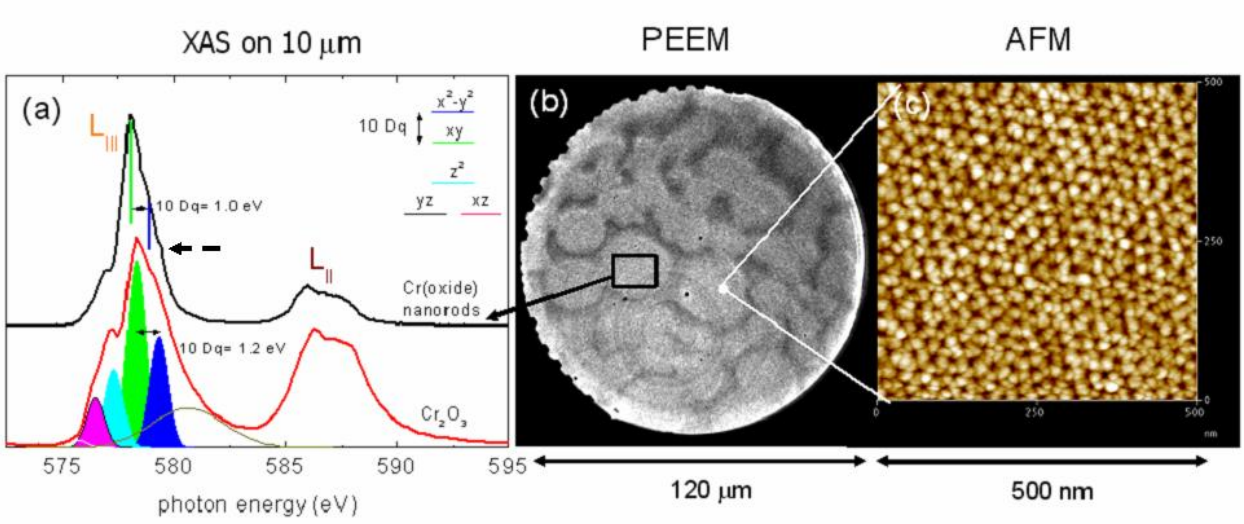

Fig. 4 Spectro-microscopy on standing chromium oxide nanorod arrays in block copolymers as performed with X-PEEM and μXAS. XAS data from the Cr LIII LII edges from chromium oxide nanorods compared with bulk Cr2O3 XAS in (a). The electronic structure with the corresponding energy levels is depicted in the right part. The crystal field split 10 Dq is extracted. The dashed arrow at 580 eV is accentuating an additional peak, caused from localisation effects due to nanostructuring. PEEM image of chromium oxide nanorod arrays in (b). The black box indicates the area of about 10 microns, the XAS spectrum in (a) was recorded from. Bright areas belong to nanorod domains in the topmost layer, darker areas are nanorod domains in the second layer, about 20 nm below the uppermost layer. Atomic force microscopy (AFM) image of standing chromium oxide nanorods in block copolymers in (c). The mesh-like structure is composed of standing chromium oxide nanorods with 8 nm diameter and 20 nm heights. Six nanorods form a hexagonal supercell with diameter of 48 nm. The AFM image was taken from the area, displayed by the white box in (b).

By a careful analysis of the unoccupied DOS as monitored with XAS from nanorod domains identified with PEEM, we find significant changes in the electronic structure of downsized chromium oxides.
In figure 4 we present μXAS, PEEM images combined with AFM. In the AFM image, displayed in figure 4(c), we resolve the lateral distribution of chromium oxide nanorods in block copolymers. Here on a scale of 500 nm we find a regular mesh-like structure composed of standing nanorods. Each single rod has a diameter of about 8 nm and a height of 20 nm. The rod-rod distance is about 20 nm and six standing rods form a hexagonal superstructure with a repetition distance of 48 nm.

On the larger length scale we identify nanorod domains with about 10-20 μm diameter in PEEM (figure 4(b)). The bright areas are composed of the complex chromium oxide nanorod and the surrounding polymer template. The darker areas between the domains are also riddled with the same kind of nanorods, only their polymeric host material lies 20 nm below the other. Therefore this PEEM image is an example for a topographic contrast, because the detection probability of electrons emitted 20 nm below others is decreased.

From one of the nanorod domains, XAS spectra were taken from the Cr L_{II} L_{III} edges and compared to data of bulk Cr_2O_3, the most stable and common oxide. One careful peak analysis was performed for both datasets to extract the electronic band structure. The unoccupied DOS of chromium oxides is derived from the t_{2g} and e_g levels, which split up in octahedrally coordinated complexes like Cr_2O_3. Due to a strong Jahn-Teller distortion the degeneracy is lifted and the states intermix and end up with yz, xz, z^2, xy and x^2-y^2 states, into which yz is completely occupied from two electrons with opposite spin and therefore not visible in XAS any more [18]. One important measure is the crystal field split 10 Dq, which

determines the energy split between different levels. 10 Dq, what is found in many textbooks about physical chemistry, determines the visible (complementary) colour of the complex [19].

For bulk Cr_2O_3 we derive 1.2 eV for 10 Dq, contrasting results for our nanopatterned chromium oxide. Here the emission lines in the L_{III} edge around 579 eV are much sharper and narrower, leading to a 10 Dq of 1.0 eV. From the sharper emissions in the L_{III} edge we can conclude, that with respect to Cr_2O_3, which is low conducting, the nanorods exhibit a higher conductivity. The line width in x-ray emission is intimately related to the screening velocity of the remaining electrons with respect to the corehole, left behind from the emitted photoelectron. Narrow peaks imply low life times of the core hole, therefore higher charge carrier mobility and as a result, a better conductivity.

Another central point in the analysis of the XAS data is the so called branching ratio L_{III} / L_{II}, the relation from the XAS emissions derived from the Cr 2p core levels [20]. The branching ratio for both spectra differs significantly due to the strongly decreased L_{II} emission intensity for nanostructured chromium rods. This signals a strong spin orbit interaction of the electrons and a higher correlated electronic band structure inside the particle with bands, showing only week dispersions [9,10].

The above effect is accompanied by a finding of a pronounced satellite peak in the high energy flank of the L_{III} emission (dashed arrow) around 580 eV, which don't have a correspondence in bulk Cr_2O_3. This is caused by the interaction of the excited electrons with new highly localized states in the band gap of the nanostructured chromium oxide [9,10,21,22].

The last case is a nice example, how X-PEEM can be used to gain new insights into nano materials. Although our PEEM image in figure 4(b) can not resolve each single nanorod, we used AFM to characterise the sample on the nanometer scale, the detection of different nanorod domains was possible by topographic contrast. By zooming inside one of these domains with XAS on the micrometer length scale, we could analyse sophisticated electronic, geometric and localisation effects induced by the nanopattering of the transition metal oxide, which establish itself in the unoccupied density of states.

4. Summary

On the last pages, and especially with the presented examples, the author has shown that an X-PEEM is a powerful diagnostic tool to evaluate complex properties of matter. When combined with synchrotron radiation the field of application extends to the so called spectro-microscopy approach with the imaging quality of a PEEM and the spectroscopic opportunities offered by XAS.

After an introduction into the principles of a PEEM and the physical origin of XA spectroscopy three examples were presented.

The first one, chromium oxide nanowires embedded into a polymeric host material were imaged with the help of a very small work function difference, allowing to distinct between the two material types, even when the nanostructures are hidden in or covered from a template.

The second example shows how X-PEEM can maybe improve the quality of conducting polymer films. Here, in the case of polyaniline, an incomplete carbon-nitrogen bond is resolved laterally and chemically, which determines the overall conductance of the thin polymer film.

The last case with standing chromium oxide nanorod arrays in polymers presents sophisticated nanopattering effects. In combination with X-PEEM and AFM single nanorods and domains composed of them were resolved and their electronic band structure is analysed with spectroscopy on the micrometer scale from one single domain.

From the listing above it is hopefully obvious, that the combination of X-PEEM and synchrotron radiation is worthy, although the technical effort is high and the number of experiments is limited.

Acknowledgements The support of D. Schmeißer (Brandenburg Technical University Cottbus (BTU) /Germany), R. Krenek and M. Stamm (Leibniz Institute for Polymer Research Dresden / Germany) is gratefully acknowledged. The Author benefited from financial support of BTU.

References

[1] J. Stöhr, and S. Anders, IBM J. Res. Develop. **44**, 535 (2000)
[2] C.R. Brundle, and A.D. Baker, *Electron Microscopy: Theory, Techniques and Applications I-V*, Academic Press (1977-1984)
[3] S. Anders, H.A. Padmore, R.M. Duarte, T. Renner, T. Stammler, A. Scholl, M.R. Scheinfeld, J. Stöhr, L. Seve, and B. Sinkovic, Rev. Sci. Instrum. **70**, 3973 (1999)
[4] R.N. Watts, S. Liang, Z.H. Levine, T.B. Lucatorto, F. Polack, and M.R. Scheinfeld, Rev. Sci. Instrum. **68**, 3464 (1997)
[5] O. Seifarth, *Properties of Chromium, Cobalt and Nickel Nanoparticles embedded into ordered Block Copolymers and Conducting Polymers*, Brandenburg Technical University Press (2006)
[6] K. Heinemann, and F. Lenz, Optik-Z. Licht u. Elektronenoptik **27**, 454 (1968)
[7] F.M.F. De Groot, J. Electron Spectr. Rel. Phen. 67, 529 (1994)
[8] G.F. Rempfer, and O.H. Griffith, Ultramicroscopy **2**7, 273 (1987)
[9] O. Seifarth, Y. Burkov, A. Goryachko, D. Schmeißer, A. Sidorenko, R. Krenek, and M. Stamm, BESSY Annual Report, 213 (2005)
[10] O. Seifarth, D. Schmeißer, R. Krenek, A. Sidorenko and M. Stamm, Progress in Solid State Chemistry **34**, 111 (2006)
[11] K. Horn, Applied Surface Science **166**, 1 (2000)
[12] O. Seifarth, R. Krenek, A. Sidorenko, I. Tokarev, S. Minko, M. Stamm, and D. Schmeißer, Thin Solid Films, in press (2007)
[13] B. Lengeler, *X-ray absorption and reflection in the hard x-ray range*, in *Photoemission and Absorption Spectroscopy of Solids and Interfaces with Synchrotron Radiation*, eds. M. Campagna, and R. Rossi, North Holland (1990)
[14] M.P. Seah, and W.A. Dench, Surface and Interface Analysis **1**, 2 (1979)
[15] J. Stöhr, *Principles, Techniques, and Instrumentation of NEXAFS in NEXAFS Spectroscopy*, Springer, Berlin, (1992)
[16] M. Magnuson, J.-H. Guo, S. M. Butorin, A. Agui, C. Sathe, J. Nordgren and A. P. Monkman, J. Chem. Phys. **111**, 4756 (1999)
[17] O. Seifarth, I. Paloumpa, and D. Schmeißer, Bessy Annual Report, 714 (2006)
[18] C. Theil, J. van Elp, and F. Folkmann, Phys. Rev. B **59**, 7931 (1999)
[19] M. Gerloch, and E.C. Constable, *Transition Metal Chemistry*, VCH, Weinheim (1994)
[20] B.T. Thole, and G. van der Laan, Phys. Rev. B **38**, 3158 (1988)
[21] R. Zimmermann, P. Steiner, R. Claessen, F. Reinert, S. Hüfner, P. Blaha, and P. Dufek, J. Phys.: Condens. Matter **11**, 1657 (1999)
[22] J. Zaanen, G.A. Sawatzky, and J.W. Allen, Phys. Rev. Lett. **53**, 418 (1985)